COUPLING MULTIPHASE HYDRODYNAMIC AND NMR PORE-SCALE MODELING FOR ADVANCED CHARACTERIZATION OF SATURATED ROCKS

N. Evseev[1], O. Dinariev[1], M. Hürlimann[2], S. Safonov[1]

[1]Schlumberger Moscow Research, 13, Pudovkina Str., Moscow 119285 Russia
[2]Schlumberger Doll Research, One Hampshire Str., Cambridge MA 02139 USA

This paper was prepared for presentation at the International Symposium of the Society of Core Analysts held in Avignon, France, 8-11 September, 2014

ABSTRACT

We use the novel method of the density functional hydrodynamics (DFH) [1 – 4] to model complex multiphase scenarios occurring in natural cores on a pore-scale. Such scenarios may be extremely diverse, ranging from those inherent in RCA and SCAL measurements, and to much more complex processes relevant to chemical EOR. We perform the numerical simulation of several multiphase flow scenarios by means of the direct hydrodynamic (DHD) simulator, which is a numerical code containing implementation of DFH. We have demonstrated some of the capabilities of our numerical tool, DHD, for simulation of multiphase flow previously [4 – 6]. Now we focus on a combination of two different methods for characterization of a multiphase system in pores. The first method comes from hydrodynamic and thermodynamic description obtained through DHD simulation. The second method emerges from numerical modeling of NMR response corresponding to T_2 relaxation and pulsed gradient spin-echo (PGSE) experiments [7 – 10], which are routinely conducted not only in laboratory, but also downhole using NMR logging tools. We model the NMR response by solving numerically the generalized Bloch-Torrey equations [11] containing relaxation, diffusion and magnetization transport terms. The equations are subject to boundary conditions describing surface relaxation. The NMR description we use enables performing modeling of T_2 relaxation and PGSE experiments, and their combination. The numerical NMR solver is also implemented within the DHD simulator. This facilitates application of NMR modeling (i.e., makes it automatic) to digitized cores with multiphase saturation, whose state has previously been described and simulated in the frame of the DFH. Such close coupling of two characterization methods different by nature is extremely important and brings an opportunity for improvement of NMR response interpretation techniques, which suffer from the inverse and ill-posed nature of the fluids characterization problem.

INTRODUCTION

The present development of pore-scale modeling of various hydrodynamic, physical and chemical phenomena is based on 3D microCT rock images, which are obtained by

different scanning techniques. With increase in resolution of X-ray and MRI methods researchers become aware of various peculiarities associated with rock microstructure as well as with consequent complexity of pore-scale processes in multiphase fluid mixtures. The fast growing body of experimental data representing the direct observation of micro- and nano-scale fluid systems makes it imperative to have more precise and physically comprehensive pore-scale models.

Recently, it has been demonstrated that a wide range of microfluidic problems can be effectively solved by the density functional hydrodynamics [3, 4, 6], which combines density functional theory with compositional multiphase hydrodynamics. DFH is able to provide detailed microscale simulation of various multiphase scenarios starting from relatively simple RCA and SCAL processes and up to very complex chemical and thermal EOR mechanisms [5]. It also covers rheology, phase transitions, partitioning and chemical reactions.

DFH is essentially a direct theory of multiphase, multicomponent mixtures. It does not rely on either phase indicator, phase saturation, order parameter or phase field; instead, it relies solely on the molar density fields of all chemical components constituting the mixture. The thermodynamic model is based on representation of Helmholtz energy or entropy as a functional depending on molar density fields. In order to account for interfacial effects this functional contains molar density gradient terms. The new system of dynamic equations obtained within the DFH framework contains equations for chemical components, equations for momentum, and an equation for total energy. This is similar to classical hydrodynamics; the difference comes from more complicated constitutive relations and boundary conditions, which are derived using explicit expressions for Helmholtz energy or entropy. Also some additional equations must be solved for complex systems containing mobile solid phases with or without structural defects.

However, being relatively complex mathematically, the DFH procedures can be parallelized on the modern CPU or even GPU-based clusters. This makes DFH computationally efficient. Another advantage of DFH is that the governing system of equations is uniform for any spatial region of interest and does not depend on specific phase content in this region. This means that the governing partial differential equations are generally the same for one-phase fluid or multiphase fluid mixture, the only difference is related to the explicit form of thermodynamic potentials.

In this paper, we study several multiphase flow scenarios using the direct hydrodynamic (DHD) simulator, which is a numerical code implementing the DFH equations. DHD is capable of modeling the following classes of multiphase hydrodynamic problems: complex compositional fluids with phase transitions (gas-liquid, liquid-liquid, liquid-solid); flow in complex geometries of boundary surfaces; wettability and adsorption; surfactants, solvents, polymers; complex fluid rheology and presence of mobile solid phase; and thermal effects. The fluid phase behavior, which is traditionally characterized by an equation of state (EoS), is converted into a thermodynamic fluid model specified by Helmholtz free energy functional, which is a principal tool in DHD. At present, high performance computing with a parallel GPU realization of the DHD code allows for simulations with several tens of billions ($\sim 10^{10}$) grid cells on a modern medium-sized

GPU cluster. The HPC version of DHD code utilizes domain decomposition parallelization method with asynchronous cross-machine communications, which gives excellent scalability and nearly linear parallel speedup. This guarantees acceptable simulation times on a today's GPU cluster systems. For example, typical computational times for complex multiphase flows in representative sub-volumes of digitized rock samples are around 1 - 3 days, while processes in simple geometries can be simulated within several minutes.

DFH can be consistently extended to take account of interaction with other non-hydrodynamic physical phenomena. One direction of development, which is outside the present paper, is the combined simulation of hydrodynamic and electromagnetic processes. Another direction of research, which is discussed in the present work, is coupling DFH to NMR. Among the multitude of NMR phenomena we consider here the magnetic response of hydrogen nuclei, which are assumed to be present in one or two fluid phases in the porous media.

We model the NMR response by solving numerically the generalized Bloch-Torrey equations containing relaxation, diffusion and magnetization transport terms. The equations are subject to boundary conditions describing surface relaxation. Since the generalized Bloch-Torrey equations contain velocity-dependent convective terms and fluid-dependent coefficients (diffusion, relaxation), the nuclear magnetization dynamics is coupled to hydrodynamics. The numerical NMR solver is implemented within the DHD simulator with parallel CPU and GPU versions. There are two ways to combine hydrodynamic and NMR simulations. First, for relatively slow hydrodynamic processes it is possible to model the evolution of the fluid distribution in pores by DFH and use a sequence of these distributions as quasi-static background states for simulation of NMR phenomena. This is important for understanding how NMR response depends on phase saturations, wettability and rock microstructure. Second, when one has relatively fast pore-scale flow, the hydrodynamics and nuclear magnetization dynamics can be both simulated in parallel by DHD. This kind of simulations can help to evaluate certain hydrodynamic properties of pore system, for example, one-phase hydrodynamic propagators.

The DHD modeling provides direct numerical solutions of hydrodynamic and NMR problems, but not the solutions of inverse problems, when NMR response is expected to characterize the actual state of rock-fluid system. Usually the complexity of inverse problems is aggravated by the ill-posed nature of the fluids characterization problem. But the study of many direct solutions can lead to better solutions of inverse problems just by fitting simulation results to experimental data. This is the overall target of coupling between pore-scale multiphase hydrodynamics and NMR theory, as it brings the opportunity for improvement of NMR response interpretation techniques.

In the present work we use DHD for modeling hydrodynamics together with T_2 relaxation and PGSE experiment, and their combination. This illustrates the potential power of NMR modeling for digitized cores with multiphase saturation, whose states have previously been described and simulated in the frame of the DFH.

This paper is the first work that addresses a coupled modeling of multiphase hydrodynamics and NMR.

RESULTS

In this section, we demonstrate numerical modeling results for three digital rock models corresponding to different natural core samples: Berea sandstone, Achimov sandstone and Cenomanian sandstone. In each case, the same modeling envelope was used. Firstly, we modeled injection of oil into initially water saturated pore space (primary drainage in water-wet case) to obtain distribution of oil at irreducible water saturation (S_{wi}). The distribution of phases thus obtained was used as an initial condition for modeling waterflooding (forced imbibition in water-wet case). The waterflooding simulation was stopped by reaching water cut limit set to 98%. Flow was arranged from bottom to top as shown in Figs. 1, 2 and 4. At the bottom side, oil or water were injected by arranging constant pressure gradient over the model, while at the top side, the outflowing liquids were taken away. The four lateral sides of the model were impermeable. Wettability was distributed over the entire surface of rock-fluid contacts using the information about contact angle measurements for each sample. To account for natural variability in contact angle, the distributions were taken to be nonuniform. . For each digital rock model, history of waterflooding was recorded so that both oil production and water cut dynamics can be analysed. As the final stage of the simulation, NMR modeling was performed to obtain DT_2 maps (diffusion – T_2 relaxation correlation) corresponding to distribution of fluids in pores before and after waterflooding. Simulation of T_2 relaxation and diffusion was conducted by solving the generalized Bloch-Torrey equations using the parameters listed in Table 1. The data from the table were assigned to each cell in accordance with the molar density distributions obtained in the multiphase flow simulations.

Table 1. Scope of data used in simulation of T_2 relaxation and diffusion

		Water	Oil
Self-diffusion, m^2/s		$2.7 \cdot 10^{-9}$	$2.1 \cdot 10^{-10}$
T_2, s		2.7	0.4
Surface relaxivity, m/s	Berea	10^{-5}	10^{-6}
	Achimov	$3 \cdot 10^{-6}$	$3 \cdot 10^{-6}$
	Cenomanian	10^{-6}	10^{-5}

Berea sandstone

We start with a very homogeneous Berea sandstone core sample. The sample was X-ray scanned with resolution 2.67 μm per voxel. The digital rock model was created with the same resolution. The model is a cube containing 500^3 identical cubic cells. Porosity of the model is 0.23 and absolute permeability is 740 mD. The fluids used in the modeling were water and decane with interfacial tension 29 mN/m. The core sample was strongly water-wet. This was modeled by assuming wettability distribution corresponding to small contact angles. The wettability was distributed stochastically and nonuniformly over the rock surface. The distribution was characterized by a correlation radius on the order of 1-2 pore sizes and the six-sigma contact angle range of $0^\circ...37^\circ$.

The rock structure of the digital rock model is presented in Fig.1a. Initially the entire pore space of the model was filled with water (Fig.1b). Decane was injected until no more water was coming out from the model. The resulting distribution of phases is shown in

Fig.1c; $S_{wi} = 0.302$. Then waterflooding of the model was performed, Fig.1d shows the distribution of water and residual decane trapped in immobile disconnected blobs. The residual decane saturation is $S_{or} = 0.253$. The chart in Fig.1e demonstrates production and water cut dynamics. After the breakthrough that happened when approximately 0.5 PV of water was pumped, water cut grew very quickly and only a small fraction of decane was produced afterwards.
Simulation results for T_2 relaxation and diffusion are presented in a form of DT_2 maps in Fig.1f,g. The first map (f) corresponds to the state of the system at the end of decane injection, while the second one (g) corresponds to the end of the waterflooding. As seen from the figures, water signal is affected by restricted diffusion and very fast T_2 relaxation caused by high surface relaxivity on the water-rock contact. All this is natural for the water-wet formations. After the waterflooding, big bodies of water appear and their presence moves the water spot closer to both bulk water diffusion and bulk T_2 relaxation values.

Achimov sandstone
The next sample we consider is Achimov sandstone taken from one of the Western Siberia fields. This sandstone is much less homogeneous than the Berea one. The resolution of the digital rock model is 2.34 μm and is equal to the X-ray scanning resolution. The model is a cube containing 700^3 identical cubic cells. Porosity of the model is 0.09 and absolute permeability is 146 mD. The fluids used in the modeling were the same water and decane used in the Berea simulations. The core sample was mixed-wet with bigger portion of the rock surface wet preferentially by water and other portions wet preferentially by decane. This was modeled by assuming wettability distribution corresponding to a wide range of contact angles. Particularly, the wettability was distributed stochastically with correlation radius on the order of 1-2 pore sizes and the resulting contact angle six-sigma range of $10^\circ...111^\circ$.
The rock structure of the digital rock model is presented in Fig.2a. Initially the entire pore space of the model was filled with water (Fig.2b). Decane was injected until no more water was coming out from the model. The resulting distribution of phases is shown in Fig.2c; $S_{wi} = 0.226$. Then waterflooding of the model was performed, Fig.2d shows the distribution of water and residual decane. The distribution of residual decane is rather complex, which results from the mixed-wet nature of the sample. The residual decane saturation is $S_{or} = 0.224$. The chart in Fig.2e demonstrates production and water cut dynamics. The breakthrough occurs after approximately 0.5 PV of water was pumped, as was the case with Berea sandstone as well. However, here the water cut does not reach the limiting value as quickly as in the Berea case. Instead, the portion of oil in the outlet drops significantly slower and it takes more than one additional PV of water (as compared to the Berea case) to be pumped through before production is stopped according to the 98% water cut criterion. Consequently, the change of slope in the production curve is also much slower.
Simulation results for T_2 relaxation and diffusion are presented in a form of DT_2 maps in Fig.2f,g. Also, for illustrative purposes, the magnetization dynamics is presented in Fig.3

by means of a series of magnetization distribution in 3D views captured at consecutive moments in time during solution of the generalized Bloch-Torrey equations. As compared to the Berea case, T_2 relaxation in water is much slower because of less influence of the surface relaxivity. At the same time, there is some influence of surface relaxivity on T_2 relaxation in oil. When after the waterflooding the amount of oil decreases, this influence becomes even stronger and also restricted diffusion becomes more pronounced in the oil signal.

Cenomanian sandstone

The third sample we consider is Cenomanian sandstone representing another one of the Western Siberia fields. This sandstone is relatively homogeneous. The resolution of the digital rock model is 2.67 μm and is equal to the X-ray scanning resolution. The model is a cube containing 400^3 identical cubic cells. Porosity of the model is 0.22 and absolute permeability is 525 mD. The fluids used in the modeling were water and oil with interfacial tension 35 mN/m. The oil was 5 times more viscous than the water. The core sample was preferentially oil-wet. The wettability map was generated stochastically with correlation radius on the order of a 1-2 pore sizes and the six-sigma contact angle range of $90^\circ...180^\circ$.

The rock structure of the digital rock model is presented in Fig.4a. Initially the entire pore space of the model was filled with water (Fig.4b). Oil was injected until no more water was coming out from the model. The resulting distribution of phases is shown in Fig.4c; $S_{\text{wi}} = 0.098$ – the smallest of all cases. Then waterflooding of the model was performed, Fig.4d shows the distribution of water and residual oil. The residual oil still fills all the small pores and sticks to the rock surface even in the bigger pores. The residual oil saturation is $S_{\text{or}} = 0.351$ – the largest of all cases. The chart in Fig.4e demonstrates production and water cut dynamics. In this oil-wet case, water breakthrough did not prevent oil from flowing because the oil cluster never becomes completely disconnected. As a result, growth of water cut is slowest among all three cases and the production process is the longest one in terms of the total liquid PVs produced.

Simulation results for T_2 relaxation and diffusion are presented in a form of DT_2 maps in Fig.4f,g. In this case, T_2 relaxation in water is almost as slow as in the bulk water. Indeed, in the oil-wet formation water tends to sit in blobs with little connection to the rock walls; therefore, its signal is almost not affected by surface relaxivity. There is influence of surface relaxivity on the oil signal, which is especially visible when compared to its counterpart in the water-wet Berea. This influence becomes even more pronounced in residual oil after the waterflooding.

CONCLUSION

We have demonstrated how DFH modeling coupled with NMR simulation can be used for advanced characterization of two-phase saturated digital rock models of cores. The modeling was used to reproduce initial saturation as well as the residual saturation obtained by direct simulation of waterflooding. Simulation takes into account

heterogeneous wettability distribution ranging from water-wet to oil-wet. All necessary properties of phases such as densities, viscosities and interfacial tension are directly entering the governing equations of DFH. After having the distributions of phases calculated, we have modeled T_2 relaxation and diffusion by directly solving the generalized Bloch-Torrey equations. The modeling takes into account bulk relaxation, diffusion and surface relaxation on the contact between rock and each of the phases. Using the simulation results, we have reconstructed DT_2 maps showing diffusion – T_2 relaxation correlation. Unlike the experimental conditions, the modeling method used here allows for establishing direct connection between particular exactly known configuration of fluids in pores and the resulting diffusion – T_2 relaxation correlation. Therefore, by comparison of the simulation results with the experimental data, the demonstrated modeling approach can be used for independent calibration of the existing NMR inversion procedures and improving of NMR logging interpretation.

ACKNOWLEDGEMENTS

We thank Schlumberger for permission to publish this work. Dmitry Koroteev, James Funk and Matthias Appel are acknowledged for reviewing the manuscript and making valuable suggestions.

REFERENCES

1. Dinariev, O., A Hydrodynamic Description of a Multicomponent Multiphase Mixture in Narrow Pores and Thin Layers. *J. Appl. Math. Mech.* 59(5), 745–752 (1995).
2. Dinariev, O., Thermal Effects in the Description of a Multicomponent Mixture Using the Density Functional Method. *J. Appl. Math. Mech.* 62(3), 397–405 (1998).
3. Demianov, A., Dinariev, O., Evseev, N., Density functional modeling in multiphase compositional hydrodynamics. *Can. J. Chem. Eng.*, V.89, April 2011, pp.206-226.
4. Demianov, A., Dinariev, O., Evseev, N., *Introduction to the density functional method in hydrodynamics*, Fizmatlit, Moscow, 2014.
5. Koroteev, D., Dinariev, O., Evseev, N., Klemin, D., Safonov, S., Gurpinar, O., Berg, S., van Kruijsdijk, C., Myers, M., Hathon, L., de Jong, H., Application of Digital Rock Technology for Chemical EOR Screening, *SPE enhanced oil recovery conference*, SPE-165258, 2013.
6. Koroteev, D., Dinariev, O., Evseev, N., Klemin, D., Nadeev, A., Safonov, S., Gurpinar, O., Berg, S., van Kruijsdijk, C., Armstrong, R., Myers, M.T., Hathon, L., de Jong, H., Direct hydrodynamic simulation of multiphase flow in porous rock, *International Symposium of the Society of Core Analysts*, SCA2013-014.
7. Hürlimann, M.D., Venkataramanan, L.. Quantitative measurement of two dimensional distribution functions of diffusion and relaxation in grossly inhomogeneous fields. *J. Magn. Reson.*, 157:31-42, (2002).

8. Hürlimann, M.D., Venkataramanan, L., Flaum, C.. The diffusion - spin relaxation time distribution function as an experimental probe to characterize fluid mixtures in porous media. *J. Chem. Phys.*, 117:10223-10232, (2002).
9. Venkataramanan, L., Song, Y.-Q., Hürlimann, M.D.. Solving Fredholm integrals of the first kind with tensor product structure in 2 and 2.5 dimensions. *IEEE Trans. Signal Processing*, 50:1017-1026, (2002).
10. Marinelli, L., Hürlimann, M.D., Sen, P.N.. Modal analysis of q-space - relaxation correlation experiments. *J. Chem. Phys.*, 118:8927- 8940, (2003).
11. Callaghan, P.T., *Principles of Nuclear Magnetic Resonance Microscopy*, Clarendon, Oxford, 1991.

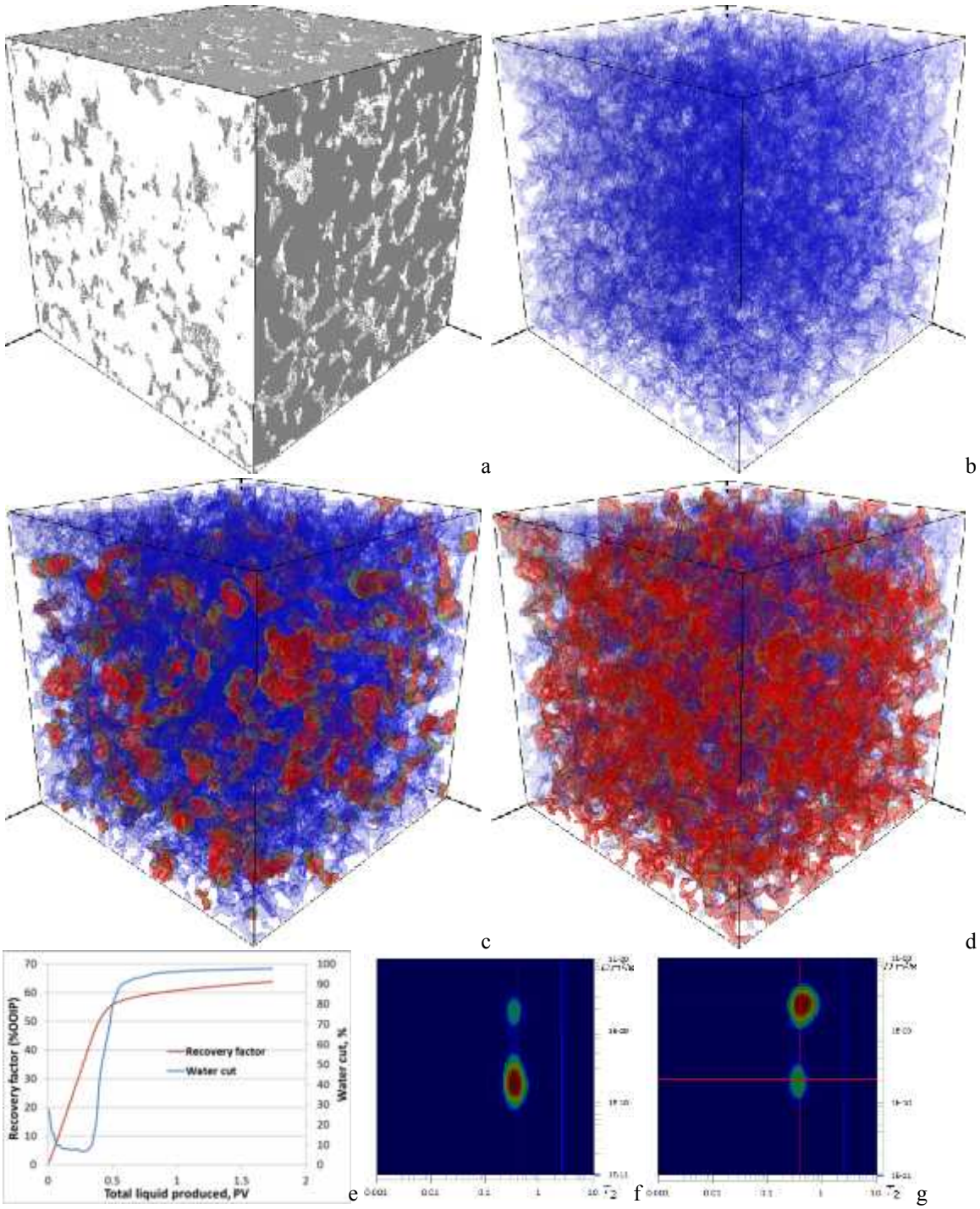

Fig.1. Berea sandstone digital rock model and numerical simulation results. Rock (a), pore space (b), distribution of water and oil after injection of oil (c) and after the waterflooding (d), oil recovery factor and water cut as functions of the total liquid produced (e), DT_2 maps corresponding to the states before waterflooding (f) and after waterflooding (g).

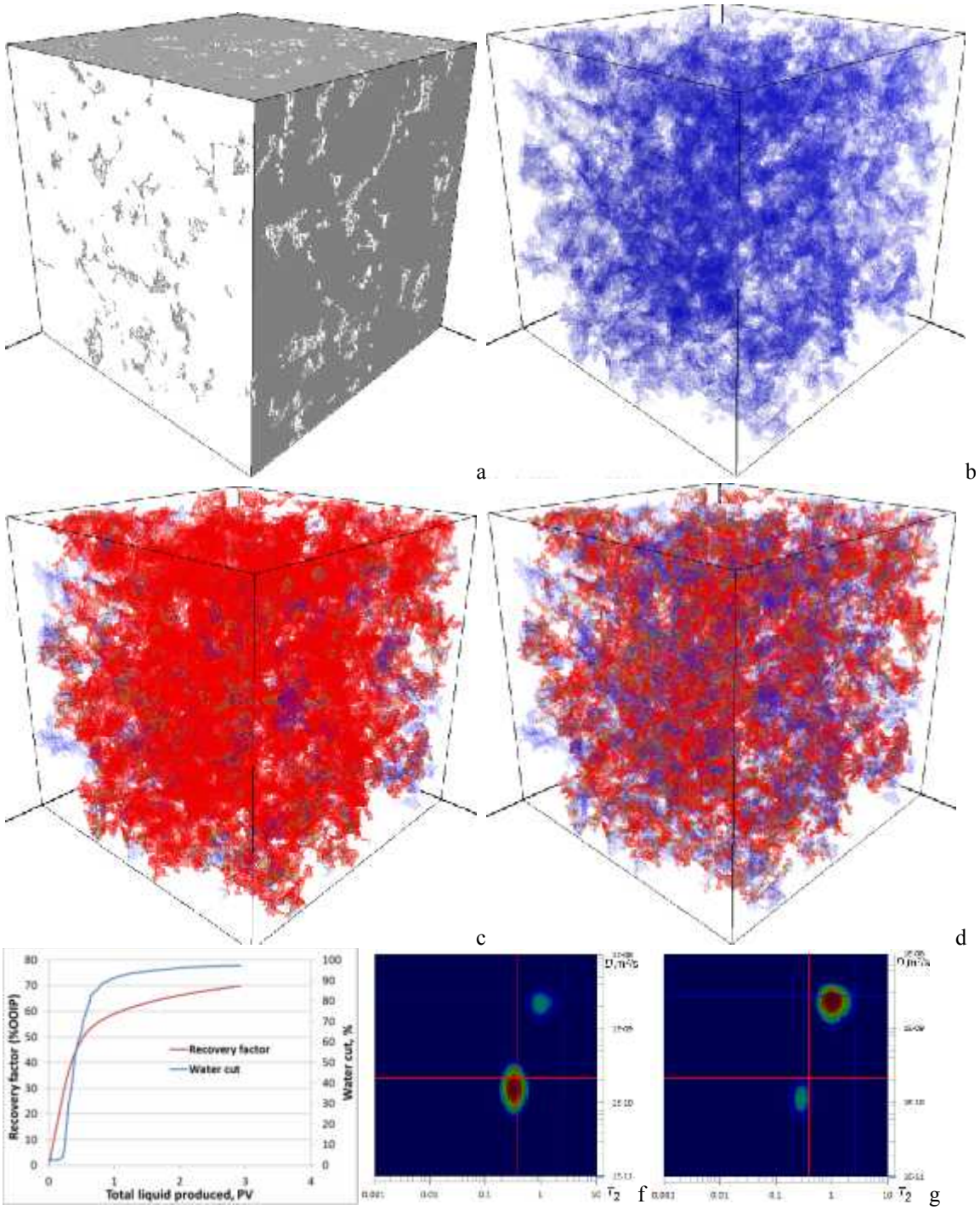

Fig.2. Achimov sandstone digital rock model and numerical simulation results. Rock (a), pore space (b), distribution of water and oil after injection of oil (c) and after the waterflooding (d), oil recovery factor and water cut as functions of the total liquid produced (e), DT_2 maps corresponding to the states before waterflooding (f) and after waterflooding (g).

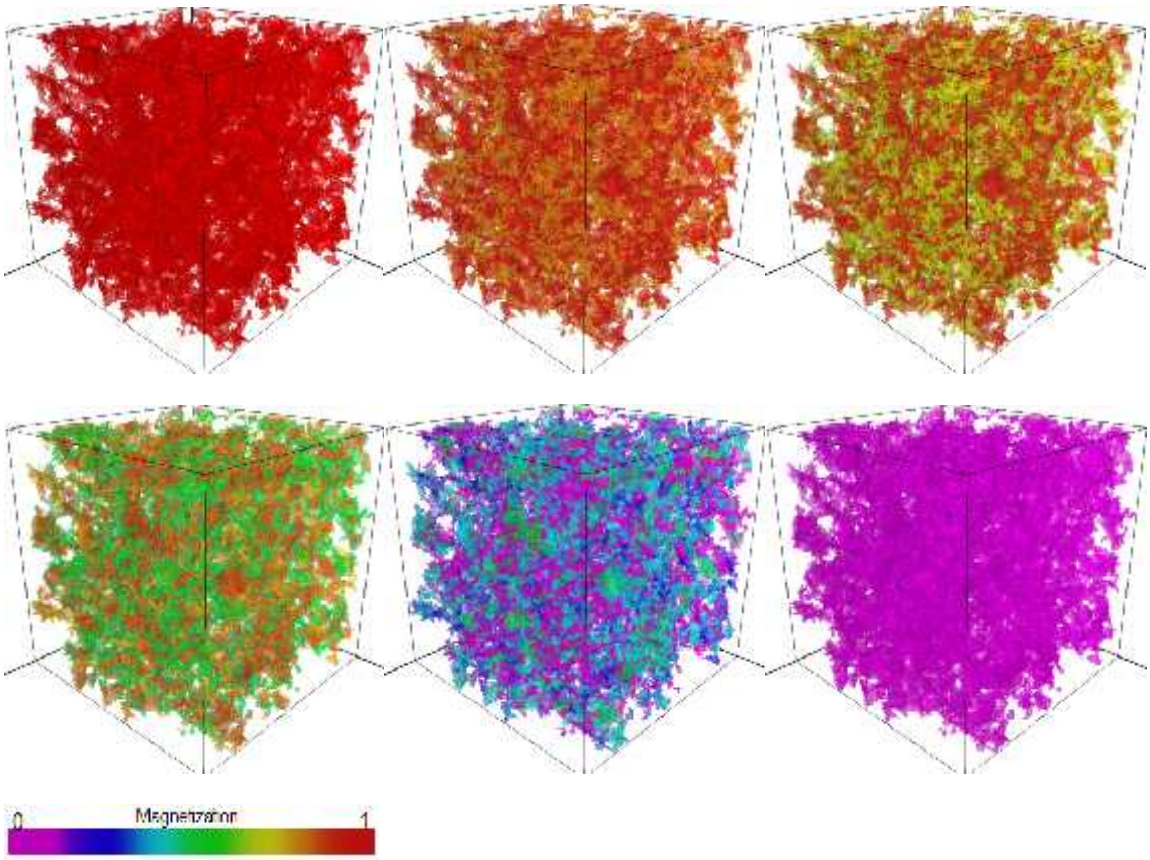

Fig.3. Magnetization decay in diffusion-relaxation simulation for Achimov sandstone. The six pictures show 3D magnetization distribution at consecutive time moments. The magnetization values were normalized to the range [0;1] and were colored according to the color palette.

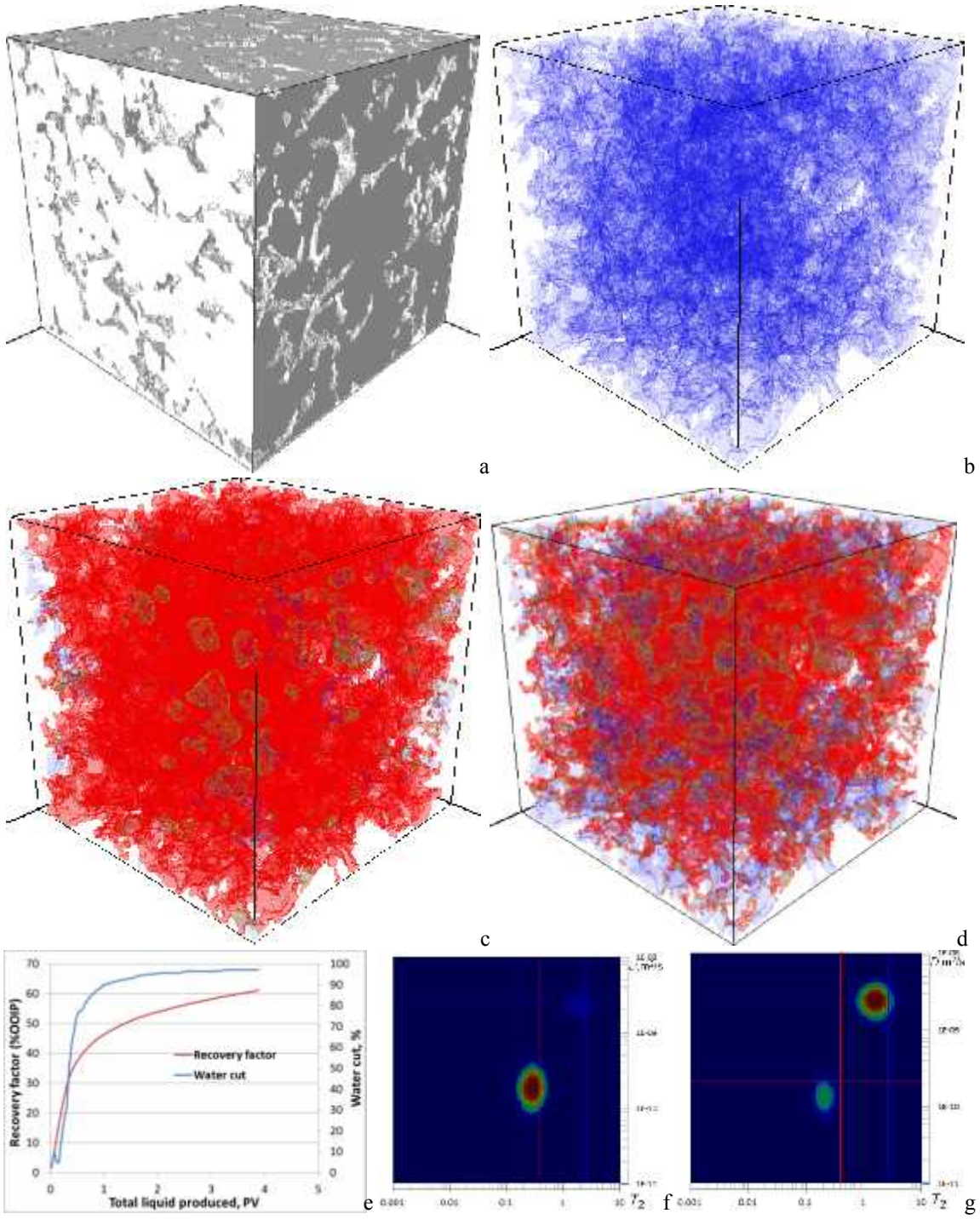

Fig.4. Cenomanian sandstone digital rock model and numerical simulation results. Rock (a), pore space (b), distribution of water and oil after injection of oil (c) and after the waterflooding (d), oil recovery factor and water cut as functions of the total liquid produced (e), DT_2 maps corresponding to the states before waterflooding (f) and after waterflooding (g).